

TIME REVERSIBLE N-BODY INTEGRATORS BASED ON SMOOTH SWITCHES

ANNE KVÆRNØ* AND BEN LEIMKUHLE**

ABSTRACT. This article describes a gravitational N-body integration algorithm incorporating the following features: (1) it is time-reversible, (2) angular and linear momentum are conserved, (3) smooth switching functions are used to split potential terms into local and weak parts so that weaker long-range forces are evaluated relatively rarely and close interactions are identified, (4) close approaches between bodies are resolved accurately, using an efficient integration method, (5) the stepsize varies automatically based on an appropriate Sundman time reparameterization. Although this method is formally second order, the most intensive computations (the close approach dynamics) are executed at a higher order, thus improving the overall accuracy of the scheme. Numerical experiments indicate that the method can effectively solve few-body gravitational problems with arbitrary two-body close approaches.

1. INTRODUCTION

The N -body problem of celestial mechanics is described by a Hamiltonian

$$\mathcal{H}(\mathbf{p}, \mathbf{q}) = T(\mathbf{p}) + f(\mathbf{q}),$$

where $T : \mathbb{R}^{3N} \rightarrow \mathbb{R}$ and $f : \mathbb{R}^{3N} \rightarrow \mathbb{R}$ are smooth kinetic and potential energy functions defined in terms of the individual momenta $\mathbf{p}_1, \mathbf{p}_2, \dots, \mathbf{p}_N \in \mathbb{R}^3$ and positions $\mathbf{q}_1, \mathbf{q}_2, \dots, \mathbf{q}_N \in \mathbb{R}^3$ of the bodies by

$$T(\mathbf{p}) = T(\mathbf{p}_1, \mathbf{p}_2, \dots, \mathbf{p}_N) := \sum_{i=1}^N \frac{|\mathbf{p}_i|^2}{2m_i},$$

and

$$f(\mathbf{q}) = f(\mathbf{q}_1, \mathbf{q}_2, \dots, \mathbf{q}_N) := - \sum_{ij} \frac{Gm_i m_j}{r_{ij}}, \quad r_{ij} = |\mathbf{q}_i - \mathbf{q}_j|,$$

1991 Mathematics Subject Classification. 65L05.

Key words. N-body problems, Hamiltonian systems, time-reversible discretization, smooth switching functions.

* Department of Mathematical Sciences, Norwegian University of Science and Technology, N-7491 Trondheim, Norway. Email: anne@math.ntnu.no

** Department of Mathematics, 405 Snow Hall, University of Kansas, Lawrence, KS 66045, USA. Email: leimkuhl@math.ukans.edu.

where G is the gravitational constant and m_i represents the mass of the i th body.

The N -body problem is the seminal problem of dynamical systems, and study of its solutions, ergodic properties, and topological structure continues to generate a great deal of mathematical and physical interest (see [16] and other recent references therein). The numerical simulation problem also remains of terrific importance. This problem is solved routinely in studies of stellar and planetary dynamics [31, 23, 1], and related problems arise in quasiclassical studies of atomic systems [24, 6, 27].

While many numerical schemes for the N -body problem have been developed over the years [9, 1], these codes may exhibit deficiencies in very long time integration or in scattering studies. One approach to improving the qualitative behavior of numerical simulation methods is to incorporate some of the many geometric properties of the phase flow, such as time-reversal symmetry, symplectic structure, and integrals such as angular momentum. Methods which preserve symmetries and invariants are sometimes referred to as *geometric* or *mechanical* integrators [25, 18, 14]. Symplectic and symmetric algorithms for smooth N -body trajectories (without close approaches) have been successfully used for long-term simulations of the solar system [31].

Close approaches introduce both theoretical and computational challenges for the Coulombic N -body problem. In the approach described here, we assume that there are potentially a large number of bodies, but at any given time only a few bodies are engaged in very close approaches. None of the geometric algorithms can be expected to preserve structure or provide substantial efficiency improvements under frequent discontinuous switchings (such as may be used for close encounters). This problem was discovered and explained by Calvo and Sanz-Serna [3] in the context of variable stepsize symplectic integration: *frequent changes in the timestepping map lead to a deterioration of the numerical stability of geometric methods*. For variable stepsizes, it turns out to be more practical to use a Sundman or Poincaré-type time-transformation to rescale the vector field or Hamiltonian in such a way that (i) geometric structure is preserved, and (ii) the new system can be solved with a fixed timestep. Articles by Stoffer [28], Hut et al [11], and the current author with collaborators [12, 10] developed the use of time-reversible variable stepsizes for N -body problems. More recently several articles have indicated how regularization methods can be incorporated in a reversible or symplectic framework [20, 15, 13].

Another approach to variable stepsize integration, based on a hierarchical splitting, was developed in [26], and we exploit this idea in a somewhat different way below, to define a *smooth switching* of the close-approaching bodies. We then separate the weaker interactions by splitting, and identify potential close approaches using *Verlet lists* [30], partitioning the bodies into small groups. The multiple timestepping framework of molecular dynamics (r-RESPA [29])

allows some control of the amount of computation performed between evaluations of the long-range forces. In order to correct for the increasing sensitivity of the dynamics of close-approaching bodies, we incorporate a Sundman time transformation using the reversible-adaptive framework developed previously by the author[15].

For problems with only two-body close approaches, much of the computational work will be in the resolution of these small systems. The switches somewhat complicate the dynamics of the two-body pairs (they are no longer pure Kepler problems). We describe an efficient technique for recovering their dynamics, based on a reduced coordinate set, a regularization, and an efficient implementation of a higher-order implicit Gauss-Legendre integrator.

When three or more body interactions in close approach must be taken into consideration (in the localized subsystem), a system of relative variables can be introduced and a regularization developed in terms of two-body pairs. In the standard approach based on Kustaanheimo-Stiefel transformation, the coupling of variables in the regularized Hamiltonian makes high-accuracy geometric integrators very costly. We suggest instead an approach based on relative coordinates, splitting, and two-body pair integration.

Our integrator could easily be adapted to the Coulombic problems arising in quasiclassical simulations of atomic systems[24, 6, 27, 15], to systems with multiple fixed bodies, or to systems subject to applied fields or arbitrary perturbing potentials, using additional splittings.

This article describes the design of the integrator. A companion article will address the implementation issues associated to this method.

2. SMOOTH SWITCHES, SPLITTING, MULTIPLE-TIMESTEPPING AND REVERSIBLE ADAPTIVE TIME-STEPPING

We use the term *smooth switch* to describe a real (backward sigmoidal) function χ which smoothly passes from one to zero in some finite subinterval of \mathbb{R}_+ :

$$\chi \in C^k(\mathbb{R}_+, [0, 1]), \quad \chi(r) = 1, \quad r < r_-, \quad \chi(r) = 0, \quad r \geq r_+, \quad \chi'(r) \leq 0.$$

Piecewise polynomial switches of any desired smoothness can be constructed as follows. First define a polynomial

$$p(x) = (-1)^{k+1} \frac{(x^2 - h^2)^{k+1}}{h^{2k+2}}.$$

This function is easily seen to satisfy the conditions $p(0) = 1$, $p^{(l)}(h) = p^{(l)}(-h) = 0$, $l = 0, 1, \dots, k$. Normalizing the integral of this polynomial on the interval $[-h, h]$ and subtracting from unity results in a new polynomial

$$q(x) = 1 - \frac{\int_{-h}^x p(x) dx}{\int_{-h}^h p(x) dx}.$$

Now for given r_- and r_+ we set $h = (r_+ - r_-)/2$, $\bar{r} = (r_+ + r_-)/2$, then the function

$$(1) \quad \chi(r) = \begin{cases} 1 & r \leq r_- \\ q(r - \bar{r}), & r_- \leq r < r_+ \\ 0, & r \geq r_+ \end{cases}$$

is a C^k switch (See Fig. 1). The fact that we can choose χ to be piecewise polynomial will be found to have some positive ramifications for the efficiency of our code.

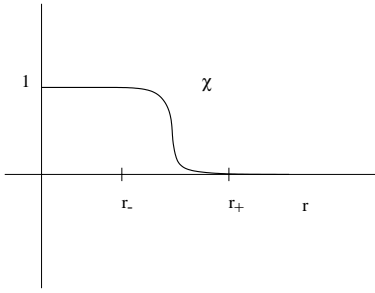


FIGURE 1. A smooth switch.

The purpose of the smooth switch is to limit the high-accuracy resolution of trajectories to close-approaching bodies, while reducing the number of force evaluations for weak interactions. We decompose each pair interaction in the gravitational potential using smooth switches:¹

$$f = \underbrace{- \sum_{ij} \chi(r_{ij}) \frac{Gm_i m_j}{r_{ij}}}_{f_{\text{loc}}} + \underbrace{- \sum_{ij} (1 - \chi(r_{ij})) \frac{Gm_i m_j}{r_{ij}}}_{f_{\text{weak}}}.$$

In a two-body problem, there are three distinct regimes in the dynamics of f_{loc} . For separations $r \leq r_-$, the dynamics are pure Keplerian. For $r \geq r_+$, the bodies are in free motion. For $r \in (r_-, r_+)$, the motion is determined by the (somewhat artificial) dynamics of the switch, integrable dynamics in a rapidly decaying force field.

To design a one-step method, we utilize a Hamiltonian splitting of the form $\mathcal{H} = \mathcal{H}_{\text{loc}} + f_{\text{weak}}$, where

$$\mathcal{H}_{\text{loc}} := T + f_{\text{loc}}.$$

¹For simplicity, we here suppose that the parameters r_- , r_+ of each switch are all identical. In many cases, it may be more practical to choose the parameters of the switch dependent on the masses of the particles of the pair. In the related classical atomic model, the switch might also depend on the product of the charges of the particle pair. This topic will be addressed in the companion article mentioned in the introduction.

Let $\Phi_{t,\mathcal{H}}$ represent the flow map on Hamiltonian \mathcal{H} , parameterized by t . We construct a splitting method using multiple time-stepping [29] with m inner substeps:

$$\Phi_{\Delta t,\mathcal{H}} \approx \hat{\Phi}_{\Delta t,\mathcal{H}} := \Phi_{\Delta t,f_{\text{weak}}} \left[\hat{\Phi}_{\frac{1}{m}\Delta t,\mathcal{H}_{\text{loc}}} \right]^m.$$

(In most cases, we would take $m = 1$, but the incorporation of multiple timestepping adds some flexibility.) Here $\hat{\Phi}_{\Delta t,\mathcal{H}_{\text{loc}}}$ is a time-reversible approximation method for solving the localized gravitational problem, as described in the next section.

The method $\hat{\Phi}_{\Delta t,\mathcal{H}}$ is a first order fixed stepsize integrator, and it is not time-reversible. We use this method as the basis for constructing a second order variable stepsize reversible integrator according to the prescription of [10]:

$$(2) \quad \begin{aligned} \begin{pmatrix} \mathbf{q}^{n+1/2} \\ \mathbf{p}^{n+1/2} \end{pmatrix} &= \hat{\Phi}_{\frac{1}{2}\Delta t_n,\mathcal{H}} \begin{pmatrix} \mathbf{q}^n \\ \mathbf{p}^n \end{pmatrix}, \\ \frac{1}{\Delta t_n} + \frac{1}{\Delta t_{n+1}} &= \frac{2}{g_{n+1/2}\Delta t}, \\ \begin{pmatrix} \mathbf{q}^{n+1} \\ \mathbf{p}^{n+1} \end{pmatrix} &= \hat{\Phi}_{\frac{1}{2}\Delta t_{n+1},\mathcal{H}}^* \begin{pmatrix} \mathbf{q}^{n+1/2} \\ \mathbf{p}^{n+1/2} \end{pmatrix}. \end{aligned}$$

where

$$g_{n+1/2} = g(\mathbf{q}^{n+1/2}, \mathbf{p}^{n+1/2})$$

and $g(\mathbf{q}, \mathbf{p})$ is the time-reparameterization function, a smooth, positive, scalar-valued function which is invariant under $\mathbf{p} \rightarrow -\mathbf{p}$ (see below). The adjoint method needed above is easily computed since $\hat{\Phi}_{\Delta t,\mathcal{H}}$ is the composition of symmetric maps:

$$\hat{\Phi}_{\Delta t,\mathcal{H}}^* = \left[\hat{\Phi}_{\frac{1}{m}\Delta t,\mathcal{H}_{\text{loc}}} \right]^m \Phi_{\Delta t,f_{\text{weak}}}.$$

Although the method is formally second-order (symmetric methods have even order [7]), we expect to utilize a higher-order integrator for the local interaction dynamics, as described in the next and following sections. Viewed as a second-order method, the scheme is therefore expected to have a relatively small leading error constant compared to a method such as Störmer-Verlet which does nothing special to integrate close approaching bodies. If desired, a third-order splitting method could be used in place of $\hat{\Phi}_{\Delta t,\mathcal{H}}$, resulting in a fourth-order method overall (see [19] for a discussion of how to construct such splittings).

We anticipate that the considerations for the choice of time-transformation will be similar to those discussed in [2, 15]. In the latter reference, it was

suggested to use a control of the form

$$(3) \quad g_{\min} = \frac{1}{1 + \bar{r}^{-3/2}}$$

where \bar{r} represents the smallest pair separation. In some cases, it may be desirable to have a smooth control, in which case we could use

$$g_{\text{sm}} = \frac{1}{1 + \left(\sum_{i < j} r_{ij}^{-3m/2} \right)^{1/m}},$$

where m is a positive integer [2]).

3. INTEGRATION OF \mathcal{H}_{loc} .

In this and the following section, we describe the integrator for \mathcal{H}_{loc} . We will assume that the solution is desired on the time interval $[0, \Delta t]$, that initial positions \mathbf{q}^0 and momenta \mathbf{p}^0 are provided and that new values \mathbf{q}^1 and \mathbf{p}^1 are to be computed.

Because of the use of switching functions, a relatively small number of the interaction terms are active in \mathcal{H}_{loc} at any given timestep; most of the particles simply drift linearly with fixed momenta. We would like to introduce the concept of a *local interaction graph* G based the positive potential interactions among the bodies. This graph will be used to limit the local computation (in the relatively expensive regularization variables) to minimal subgroups of bodies. However, there is some question about how to define G . Clearly the vertices of G are the body indices, but what should we take for the edges?

Given vertices i and j , it is evidently not sufficient to add the edge $\bar{i}\bar{j}$ only when $\|\mathbf{q}_i^0 - \mathbf{q}_j^0\| \leq r_+$, since, during the timestep, the two bodies may move closer to each other and thus have a close interaction by the end of the timestep. Moreover, the one-step methods we propose for integrating the few-body problems will evaluate the forces at an intermediate point in the subinterval. Still it is not sufficient to simply link i and j based on the initial, final and intermediate steps, since it is necessary to know these interactions *at the start* of the timestep (after all, the whole purpose of constructing the graph is to restrict the computation to local groups!). To define the interaction graph, we therefore need a very cheap method to predict, based only on the initial positions and velocities, which particles have the potential to have a local interaction during the current timestep. The same technique used to construct *Verlet lists*[30] in molecular dynamics can be used for this purpose.

To identify potential close approaches, we proceed as follows for each of the i bodies (being careful to work with squared norms to avoid computation of extra square roots). We iterate over the bodies with index $j > i$. Define

$$\Delta \mathbf{q} = \mathbf{q}_i^0 - \mathbf{q}_j^0, \quad \Delta \mathbf{p} = \mathbf{p}_i^0 - \mathbf{p}_j^0,$$

We first compute $\sigma^0 = |\Delta \mathbf{q}|^2$. Clearly if $\sigma^0 < r_+^2$, we should add edge \bar{ij} to G , but because our method is heuristic (based only on linear trajectories), we include a relaxation factor $\beta > 1$ and check instead $\sigma^0 < \beta r_+^2$. Next, we compute the time of close approach of the linear trajectories through $(\mathbf{q}_i^0, \mathbf{p}_i^0)$, $(\mathbf{q}_i^1, \mathbf{p}_i^1)$, $(\mathbf{q}_j^0, \mathbf{p}_j^0)$ and $(\mathbf{q}_j^1, \mathbf{p}_j^1)$.

$$t^* = -\frac{\Delta \mathbf{q} \cdot \Delta \mathbf{p}}{|\Delta \mathbf{p}|^2}.$$

If $t^* \in [0, \Delta t]$, then we compute the squared separation between these two trajectories at t^* , $\sigma^* = |\Delta \mathbf{q} + t^* \Delta \mathbf{p}|^2$, and check if $\sigma^* < \beta r_+^2$. Finally, we compute the separation at the right endpoint of the time interval, $\sigma^1 = |\Delta \mathbf{q} + \Delta t \Delta \mathbf{p}|^2$, adding the edge if this is less than βr_+^2 .

After updating the interaction graph, we subdivide the indices $1, 2, \dots, N$ into L disjoint connected components $\Omega_1, \Omega_2, \dots, \Omega_L$. These components will generally consist of one or several indices. The cost of resolving the close approaches rises very rapidly with the number of bodies, while the attainable accuracy diminishes, but close approaches of three or more bodies are rare. In the next section we focus on the case of two-body approaches. Later, we will describe a method for handling higher-body collisions.

4. FAST INTEGRATOR FOR THE SWITCHED PROBLEM: TWO-BODY CASE

The computation of the close encounters is typically the most costly part of the calculation, so substantial algorithmic effort is warranted in the interest of overall efficiency. In this section we describe a technique for two-body approaches based on polar coordinates in the plane of motion, regularization, and the Gauss-Legendre family of higher-order implicit Runge-Kutta methods.

Any Hamiltonian system of the form

$$H_{2bdy} = \frac{1}{2m_1} |\mathbf{p}_1|^2 + \frac{1}{2m_2} |\mathbf{p}_2|^2 + \phi(|\mathbf{q}_1 - \mathbf{q}_2|)$$

is integrable. For Kepler's problem, an elegant solution was known at least to Gauss, and is detailed in [17]. A number of papers have considered efficient numerical methods for solving the associated nonlinear equation (see e.g. [21, 22]). A method avoiding all transcendental functions was used in [15], based on implicit midpoint applied in the Kustaanheimo-Stiefel variables, but this scheme may not provide sufficient accuracy in some cases.

Solutions for special cases of the two-body problem with various power potentials are discussed in [5], however for *arbitrary* ϕ , the computation of the associated quadrature and nonlinear equations becomes complicated by potential singularities and a sign change of the integrand, and an involved procedure is then needed to perform the computations, including a special quadrature algorithm and case-dependent changes of variables.

Converting to relative coordinates, rotating the plane of motion (with normal $\mathbf{n} = (\mathbf{q}_1 - \mathbf{q}_2) \times (\mathbf{p}_1 - \mathbf{p}_2) = \text{constant}$) onto the xy coordinate plane, and then introducing polar coordinates gives the Hamiltonian

$$H_{\text{plane}} = \frac{1}{2\bar{m}} p_r^2 + \frac{1}{2\bar{m}} \frac{l^2}{r^2} + \phi(r)$$

where $l = p_\theta$ is the local angular momentum of the particular approaching pair. Again, this gives an integrable system. To solve it, we could proceed to recover the solution by piecing together solutions of the separable scalar ODE

$$\frac{d}{dt}r = \pm \sqrt{2\bar{m} \left(E_0 - \phi(r) - \frac{l^2}{r^2} \right)},$$

where $E_0 = H_{\text{plane}}$ is the energy of the reduced problem. The numerical solution of this differential equation in terms of quadratures is challenging and inefficient. Not only do we have to design an accurate numerical quadrature subject to a switching of sign, but the solution is then only obtained in implicit form, defined by a certain nonlinear equation. Observe also that there is nothing to prevent $l = 0$, thus arbitrarily close approaches of the bodies (or even collisions) are indeed possible, causing a singularity in the integrand. Despite these problems, a viable method for the general case could undoubtedly be derived based on quadrature, but we are skeptical that it would be as efficient and robust as the alternative we describe in the sequel.

The canonical equations of H_{plane} are

$$\begin{aligned} \frac{d}{dt}r &= \frac{1}{\bar{m}} p_r \\ \frac{d}{dt}p_r &= \frac{1}{\bar{m}} \frac{l^2}{r^3} - \phi'(r) \\ \frac{d}{dt}\theta &= \frac{1}{\bar{m}} \frac{l}{r^2} \end{aligned}$$

By introducing a new variable $\eta = r \cdot p_r$, performing a Sundman transformation $dt/d\tau = r$, and taking advantage of the constant energy, this system can be written as

$$(4) \quad \frac{d}{d\tau}r = \frac{1}{\bar{m}}\eta$$

$$(5) \quad \frac{d}{d\tau}\eta = 2rE_0 - 2r\phi(r) - r^2\phi'(r)$$

$$(6) \quad \frac{d}{d\tau}t = r$$

$$(7) \quad \frac{d}{d\tau}\theta = \frac{1}{\bar{m}} \frac{l}{r}$$

These equations are no longer canonical, however, the symmetry of the original system is retained. The first three of these equations can be solved independent

of the last one. And, since $\phi(r) = -\gamma/r \cdot \chi(r)$, $\chi(r)$ piecewise polynomial, all singularities have been removed from (4)-(5), thus, at least theoretically, they can be solved even through head-on collisions.

The solution of the regularized equations (4)-(7) requires an accurate and stable geometric integration method such as the efficiently implemented Gauss-Legendre method described below.

High order is needed in this step because the regularization process (absolutely essential to stable integration) introduces the energy of the two-body problem as a parameter of the differential equations, hence upsetting the iterated-map property which guarantees structural stability properties such as orbital symmetry [15]. Only in the case of a pure Kepler problem is the regularized Hamiltonian quadratic, hence conserved by the Gauss methods [4]. Especially in the switching regime of our two-body potential, the energy may fluctuate significantly, thus a high-order method is required.

A GAUSS-LEGENDRE METHOD FOR THE REGULARIZED REDUCED PROBLEM.

We will here briefly describe the implementation of a fully implicit Runge-Kutta method applied to the regularized problem (4)-(7). A discussion of implementation issues for general ordinary differential equations can be found in [8, IV.8]. In this section, we concentrate on issues specific to the given problem, which in the sequel will be written as

$$(8) \quad \frac{d^2}{d\tau^2}r = \frac{1}{\bar{m}}f(r), \quad \frac{d}{d\tau}t = r, \quad \frac{d}{d\tau}\theta = \frac{1}{\bar{m}}\alpha(r) \quad \text{and} \quad \eta = \bar{m} \frac{d}{d\tau}r$$

These equations are solved by some (possibly) high order Gauss-Legendre methods [8, IV.5]. Using the standard Butcher notation, the coefficients in an s -stage method are given by a matrix $\mathbf{A} = (a_{ij})_{i,j=1}^s$ and vectors $\mathbf{b} = (b_1, b_2, \dots, b_s)^T$ and $\mathbf{c} = (c_1, c_2, \dots, c_s)^T$. Applied to (8), it results in the following system of nonlinear equations, (\hat{a}_{ij} being the elements of the matrix \mathbf{A}^2):

$$(9) \quad R_i = r_n + \frac{1}{\bar{m}}c_i\Delta\tau\eta_n + \frac{1}{\bar{m}}\Delta\tau^2 \sum_{j=1}^s \hat{a}_{ij}f(R_j), \quad i = 1, 2, \dots, s$$

and the solution is updated by

$$(10) \quad t_{n+1} = t_n + \Delta\tau \sum_{i=1}^s b_i R_i$$

$$(11) \quad r_{n+1} = r_n + \Delta\tau \frac{1}{\bar{m}} \eta_n + \frac{1}{\bar{m}} \Delta\tau^2 \sum_{i,j=1}^s b_i a_{ij} f(R_j)$$

$$(12) \quad \eta_{n+1} = \eta_n + \frac{1}{\bar{m}} \Delta\tau \sum_{b_i} f(R_i)$$

$$(13) \quad \theta_{n+1} = \theta_n + \frac{1}{\bar{m}} \Delta\tau \sum_{i=1}^s b_i \alpha(R_i)$$

A curious twist is that the timestep $\Delta t_n = t_{n+1} - t_n$ is known, but the corresponding fictive timestep $\Delta\tau$ must be computed. Thus (9) and (10) must be solved for R_1, \dots, R_s and $\Delta\tau$ simultaneously. Newton iteration techniques will normally be adequate. The Jacobian matrix of this system of $s + 1$ nonlinear equations can be written in block form,

$$\mathbf{J} = \begin{pmatrix} \hat{\mathbf{J}} & \mathbf{v} \\ \mathbf{u}^T & w \end{pmatrix}$$

where the elements of the $s \times s$ -matrix $\hat{\mathbf{J}}$ are

$$J_{ij} = \delta_{ij} - \frac{\Delta\tau^2}{\bar{m}} \hat{a}_{ij} g'(R_j)$$

where δ_{ij} is 1 if $i = j$ and otherwise zero, \mathbf{v} has elements

$$v_i = -\frac{1}{\bar{m}} c_i \eta_n - \frac{2}{\bar{m}} \Delta\tau \sum_{i,j=1}^s \hat{a}_{ij} f(R_j),$$

$\mathbf{u} = -\Delta\tau \mathbf{b}^T$ and $w = -\sum_{i=1}^s b_i R_i$. The Jacobian can be computed in the beginning of each step, and then held fixed during the iterations. Having a good predictor is critical for the overall success of the method. One option is to use a high-order Taylor series approximation, obtained through differentiation of the differential equation. This is especially viable because the function $f(r)$ is piecewise polynomial. Extrapolating values from a previous step (using the collocation polynomial) is inadvisable since the integration of (8) over one (outer) step is only a part of the overall algorithm, thus the right hand side of the equation changes from step to step. For the same reason, the Jacobian cannot be kept fixed over several steps.

For very close encounters, the Jacobian \mathbf{J} tends to become singular, and special care has to be taken for the solution of the nonlinear equations. (This and other implementation issues will be taken up in a companion paper article.)

Since the energy E_0 is used as a parameter in the regularized equations, time symmetry is not really retained. However, since high order methods are used, we are willing to accept this small destruction of time symmetry. In fact, as we will show later, experiments shows that this discrepancy in energy has less effect on the time symmetry than the floating point errors introduced when solving the unregularized equations.

5. HIGHER-BODY CLOSE ENCOUNTERS

We next briefly consider numerical integrators for the case that a component of the local interaction graph can include three or more bodies. The equations in this case are no longer integrable, so the only possibility is to derive an appropriate numerical discretization scheme. In general, our problem is to integrate numerically an d -body problem with Hamiltonian of the form

$$\frac{1}{2} \sum_{i=1}^d \frac{|\mathbf{p}_i|^2}{m_i} + \sum_{j=1}^{d-1} \sum_{k=j+1}^d \phi(|\mathbf{q}_i - \mathbf{q}_j|)$$

Due to our use of splitting and time-transformation, we can restrict attention to the case where the number of bodies d is small.

As is the usual practice, we first introduce relative coordinates for the pair separations,

$$\begin{aligned} \boldsymbol{\delta}_1 &= \mathbf{q}_1 - \mathbf{q}_2, & \boldsymbol{\delta}_2 &= \mathbf{q}_1 - \mathbf{q}_3, & \dots, & \boldsymbol{\delta}_{d-1} &= \mathbf{q}_1 - \mathbf{q}_d, \\ & & \boldsymbol{\delta}_d &= \mathbf{q}_2 - \mathbf{q}_3, & \dots, & \boldsymbol{\delta}_{2d-3} &= \mathbf{q}_2 - \mathbf{q}_d, \\ & & & & \dots, & \boldsymbol{\delta}_{\frac{1}{2}(d^2-d)} &= \mathbf{q}_{d-1} - \mathbf{q}_d. \end{aligned}$$

Together with the center of mass, these variables, though degenerate ($D = (d^2 - d)/2 \geq d, d \geq 3$), are adequate to describe any configuration. Canonical equations can be developed in terms of the relative variables, by introducing suitable momenta $\boldsymbol{\pi}_i$ canonically conjugate to the $\boldsymbol{\delta}_i$. Neglecting the center of mass motion, the Hamiltonian becomes

$$H_{\text{rel}} = \frac{1}{2} \sum_{i=1}^D \frac{|\boldsymbol{\pi}_i|^2}{2\bar{m}_i} + \sum_{j \neq k} \sigma_{jk} \boldsymbol{\pi}_j \cdot \boldsymbol{\pi}_k + \sum_{i=1}^D \phi(|\boldsymbol{\delta}_i|),$$

where $\bar{m}_i = 1/(1/m_\alpha + 1/m_\beta)$, where m_α and m_β are the masses of the bodies of the i th pair, and σ_{jk} is either zero (if the pairs on which $\boldsymbol{\delta}_j$ and $\boldsymbol{\delta}_k$ are based involve no common body) or else \pm the reciprocal of the common mass of the j th and k th pairs of bodies, depending on the order of the differences.

Now there are several ways to proceed. A traditional course, described concisely in [20], is to apply the Kustaanheimo-Stiefel regularizing transformation to all the variables. The kinetic energy metric is then position dependent and rather complicated. The nonseparable nature of the Hamiltonian precludes the use of (known classes of) explicit geometric integrators, leaving us essentially

with implicit methods such as the Gauss-Legendre Runge-Kutta methods or Lobatto IIIA-B partitioned Runge-Kutta pairs[7], but in this case, there are no simple reductions of the numbers of variables such as we found in the previous section. For example, a fourth-order method for the three-body problem would require the solution of a nonlinear system of dimension $2 \times 24 = 48$ at each step. This is clearly unacceptable in long-term simulations, for which many such nonlinear systems may need to be solved.

Instead, we will look for a splitting of H_{rel} that requires only the solution of two-body problems at each step. The numerical method of the previous section can then be used to solve the two-body problems.

One such splitting would break H_{rel} into two parts,

$$H_{\text{rel}} = H_1 + H_2,$$

where

$$H_1 = \sum_{i=1}^D \frac{|\boldsymbol{\pi}_i|^2}{2\bar{m}_i} + \sum_{i=1}^D \phi(|\boldsymbol{\delta}_i|),$$

and

$$H_2 = \sum_{j \neq k} \sigma_{jk} \boldsymbol{\pi}_j \cdot \boldsymbol{\pi}_k.$$

H_1 consists of D decoupled two-body problems, whereas H_2 is only P dependent, hence both terms are integrable.

An alternative splitting method would divide H into D parts,

$$H_{\text{rel}} = G_1 + G_2 + \dots + G_D$$

where

$$G_i = \frac{|\boldsymbol{\pi}_i|^2}{2\bar{m}_i} + \phi(|\boldsymbol{\delta}_i|) + \frac{1}{2} \sum_{k \neq i} \sigma_{ik} \boldsymbol{\pi}_i \cdot \boldsymbol{\pi}_k.$$

Each of the D terms can be seen to be integrable, since only the i th momentum vector changes during the integration of G_i . In the case of a 3-body problem, this splitting has three terms. For higher order, the number would rapidly increase.

Both splittings are easily seen to conserve angular momentum, since each of the terms has this feature and the discretization is constructed by concatenation of the exact flows (or conserving approximations of the exact flows) on each term.

To obtain higher-order methods, we suggest to use the concatenation technique [32, 19, 25]. For the alternative decomposition, second and fourth order splitting methods are also easily derived.

6. NUMERICAL EXPERIMENTS

In the experiments described below, we have used an adaptive Verlet-Leapfrog method, one step with the method is given by

$$\Phi_{\frac{1}{2}\Delta t_n, f_{\text{weak}}} \circ \hat{\Phi}_{\Delta t_n, \mathcal{H}_{\text{loc}}} \circ \Phi_{\frac{1}{2}\Delta t_n, f_{\text{weak}}}.$$

The stepsize is updated between the steps, using (2) with $g = g(\mathbf{q}^n, \mathbf{p}^n), g$ given by (3)². For close encounters, $\hat{\Phi}_{\Delta t_n, \mathcal{H}_{\text{loc}}}$ is solved by an eight order Gauss method, as described. In the experiments, we compare

(a) the variable stepsize leapfrog method without a switch

with the same method using:

(b) a hard switch, meaning that the switch is turned on, that is $\chi = 1$, whenever $r < \bar{r}$ in the beginning of the step, otherwise the switch is turned off.

(c) an improved hard switch, in which linear extrapolation is used to decide whether r is less than \bar{r} over the whole step, in which case the switch is turned on.

(d) the smooth switch (1) with $k = 8$.

For the variable stepsize method, the fictive stepsize was $\Delta t = 0.04$. For the smooth switch we have used $r_+ = 0.02$, $r_m = r_+/8$, and for the hard switches $\bar{r} = (r_+ + r_-)/2$.

Example 1: The Kepler problem.

Our first example, the two-dimensional Kepler problem, has been chosen to demonstrate the reliability of the smooth switch for solving two-body close encounters. The Hamiltonian is

$$H = \frac{1}{2}(p_1^2 + p_2^2) - \frac{1}{\sqrt{q_1^2 + q_2^2}}$$

As initial values we choose

$$q_1(0) = 1 + e, \quad q_2(0) = 0, \quad p_1(0) = 0, \quad p_2(0) = \sqrt{(1 - e)/(1 + e)}$$

thus the solution (q_1, q_2) forms an ellipse with eccentricity e , $0 \leq e < 1$, and with period 2π . The smallest distance from the origin is $r_{\min} = 1 - e$. The system with $e = 0.9999$ was integrated over 32 periods. The average stepsize used by the algorithms was about 0.01.

The superiority of the smooth switch is clearly demonstrated by Figures 2 and 3. The adaptive leapfrog without switch suffers from a phase shift caused by the high energy in the close domain. The hard switches partly eliminate that phase shift, but a severe drift in the energy error is introduced. The combination of leapfrog and the smooth switch eliminates the secular drift in both phase and energy.

²After the first half step, this is equivalent to the symmetric adaptive Verlet method [10].

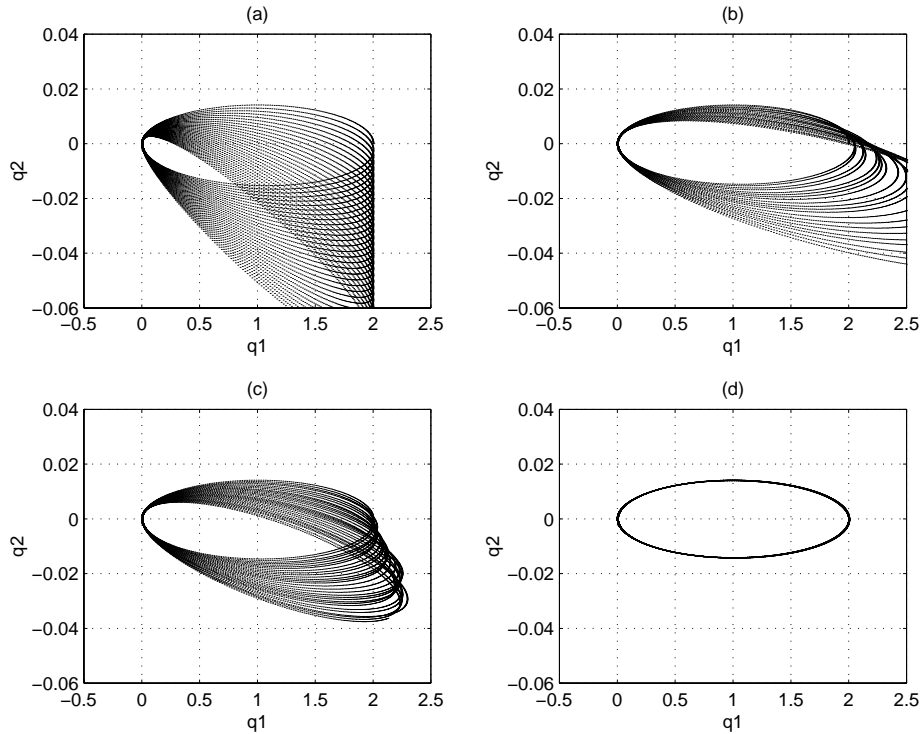


FIGURE 2. The orbit of the Kepler problem ($e=0.9999$) solved by the variable stepsize leapfrog method (a) without switch, with (b) hard switch, (c) improved hard switch and (d) smooth switch.

Figure 4 illustrates how the energy varies over one period. To better visualize the behaviour of the methods within the close domain, the energy error is shown as functions of the number of steps. For comparison, the energy fluctuations for two eccentricities, $e = 0.9999$ and $e = 0.999999$, are shown. We can clearly see how the switches “cut the peak” off the energy error of the leapfrog method. The hard switches are, however, unable to regain the energy level when out of the close domain, a problem that gets worse for higher eccentricities. It is also interesting to notice that the energy error for the smooth switch is almost independent of the eccentricity. However, the smooth switch creates fluctuations in the switching regime. Experiments show that these fluctuations become worse when r_+ and r_- are close to each other.

It is also of interest to see how the switches affect the time symmetry. To this end, the Kepler problem is integrated forward one period, and then backward using the same stepsize sequence. Figure 5 shows the norm of the displacement of \mathbf{q} caused by this process for several choices of $r_{\min} = 1 - e$. Thus, for r_{\min} less than r_+ (or \bar{r} for the hard switches), the orbit is always outside the switching regime. However, when in effect, the simple hard switch (\star) destroys the time

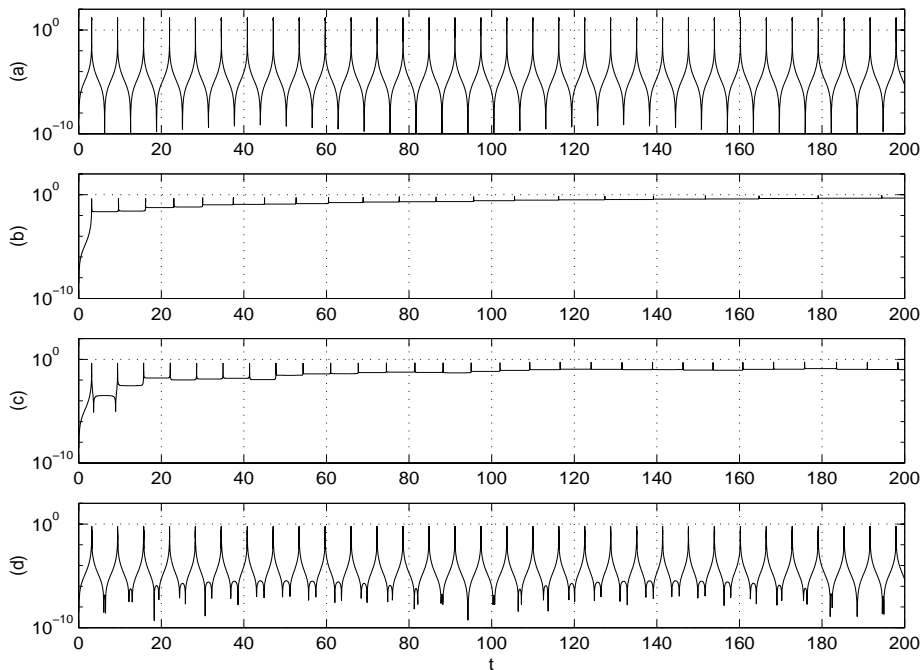


FIGURE 3. The relative energy error in simulation of the Kepler problem ($e = 0.9999$). (a) Without switch, with (b) hard switch, (c) improved hard switch and (d) smooth switch.

symmetry completely. It is also interesting to note that the method without switches (\times), which is known to retain, formally, time symmetry, loses this property in practice.

This is caused by large rounding errors introduced in solving the unregularized equations close to the singularity. The smooth switch (\circ), as well as the improved hard switch ($+$) retains the time symmetry fairly well. Thus, it seems that the benefits of solving the regularized equations, outweigh the disadvantage of the energy error introduced in the switching regime.

Even if time symmetry is retained fairly well for the hard switch, we have already seen that the numerical solution produced by this method shows a quite irregular behaviour. This is because preservation of geometrical properties relies on the existence of modified equations, a system of differential equations whose exact solution agrees with the numerical solution to some order. Because of the discontinuities introduced by the hard switches, no modified equations exist.

Finally, Figure 6 shows the development of the global error in \mathbf{q} . As expected, both the method without the switch and the method with a smooth switch show linear error growth, although the error of the latter is only about

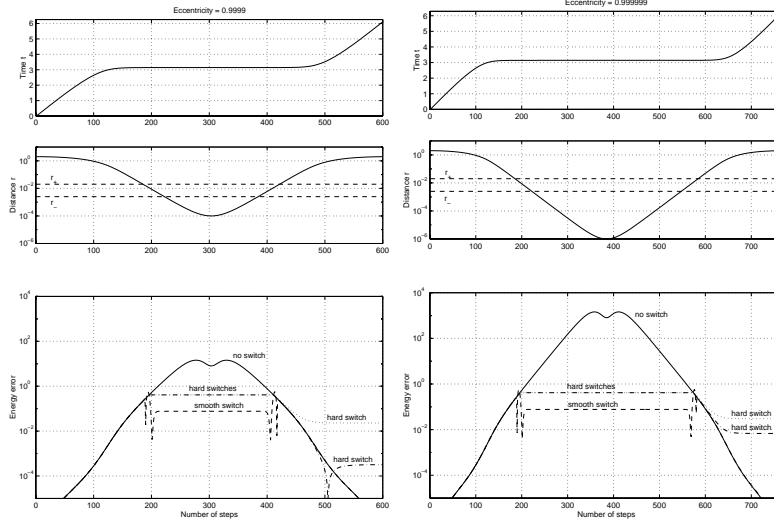


FIGURE 4. The distance r and the energy error over one period for the variable stepsize method without switch (- -), with hard switch ($\cdot\cdot\cdot$), improved hard switch ($\cdot-$) and smooth switch (-).

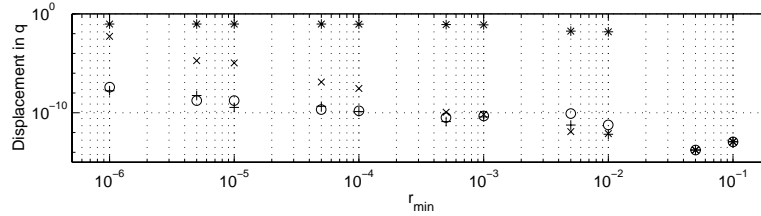


FIGURE 5. The displacement of q after integrating forward one period, and then backward again, without switch (\times), with hard switch (\star), improved hard switch ($+$) and smooth switch (\circ).

20% of the first one. The hard switches give no such regular behaviour of the growth of the global error, further, the size of the errors is quite alarming.

Example 2: Attraction by two fixed centres.

Our next example is the problem of attraction by two fixed centres, located at $(-0.5, 0)$ and $(0.5, 0)$. The Hamiltonian is

$$H = \frac{1}{2}(p_1^2 + p_2^2) - \frac{1}{\sqrt{(q_1 - 0.5)^2 + q_2^2}} - \frac{1}{\sqrt{(q_1 + 0.5)^2 + q_2^2}}$$

and the initial values used are

$$q_1(0) = q_2(0) = 0, \quad p_1(0) = p_2(0) = 0.8$$

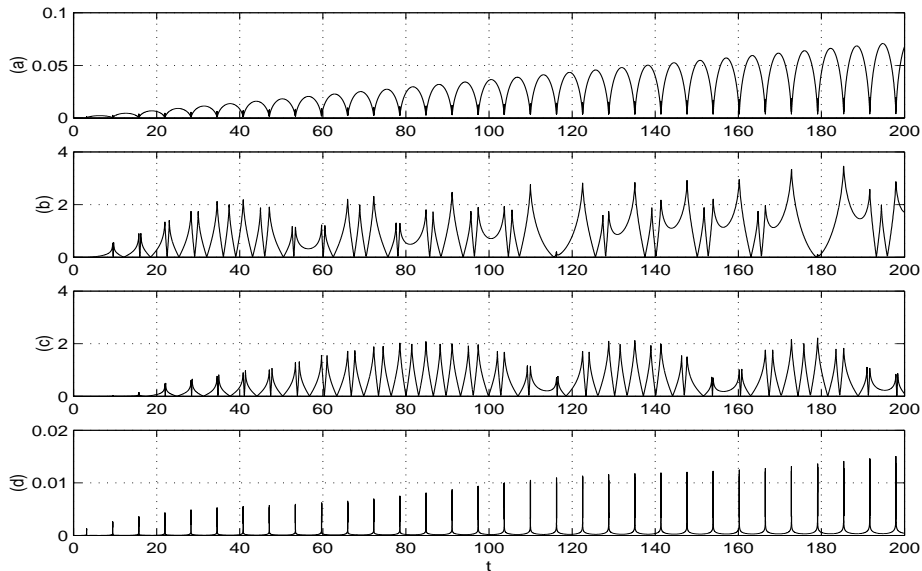


FIGURE 6. The global error in simulation of the Kepler problem ($e = 0.9999$). (a) Without switch, with (b) hard switch, (c) improved hard switch and (d) smooth switch.

The problem has been solved without switch, with the improved hard switch and with the smooth switch. The results are shown in Figures 7 and 8. The “exact” solution has been found by integrating the problem with an explicit Runge-Kutta method (MATLABs ODE45) with very strict tolerances ($1.e-12$). Again, we can see how the switches remove the energy peaks of the adaptive leapfrog method. However, there is again a drift in the energy for the hard switch. No such drift can be observed for the smooth switch. Although it is hard to give a clear measure of the quality of the solution, Figure 7 clearly shows that the smooth switch retains the ergodic behaviour better than the other two methods.

7. DISCUSSION

In this paper, we have presented a gravitational N-body integration algorithm. Smooth switching functions have been used to split the potential terms into local and weak parts. Close approaches between bodies are solved through a regularized system of equations, using a high order Gauss method. Numerical experiments clearly demonstrate the superior qualitative behaviour of the proposed algorithm, however, the integration of close encounters is quite costly. This can still be justified since close encounters normally happen relatively

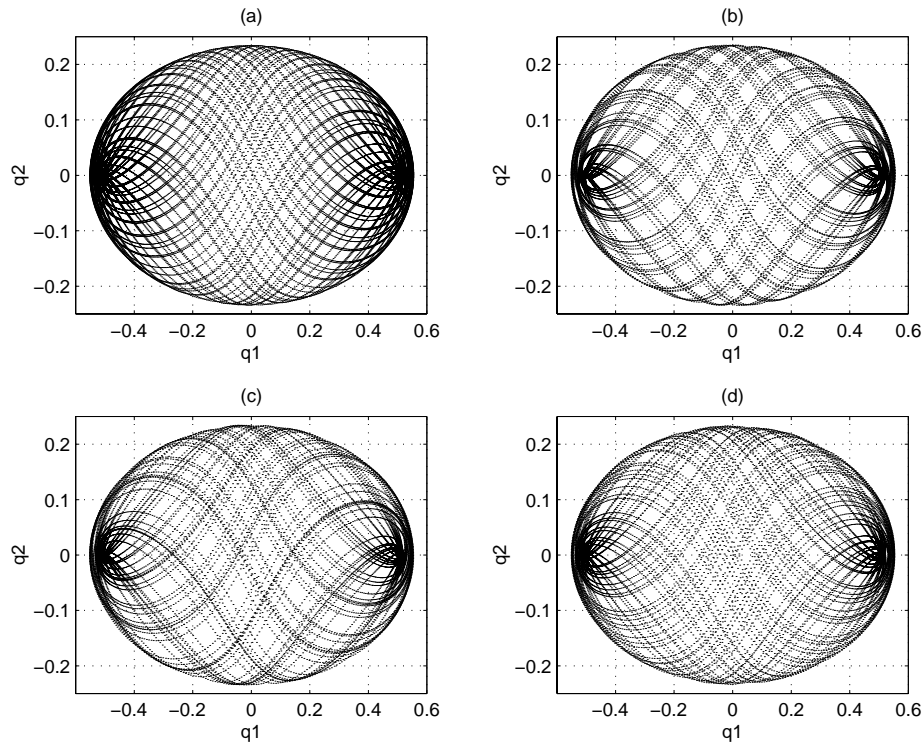


FIGURE 7. The orbit of Example 2, solved (a) exact, (b) without switch, (c) with improved hard switch and (d) with smooth switch.

rarely: in Example 2, about 20% of the steps were taken within the switching regime. This number can be reduced by reducing the switching regime, thus a correct choice of r_+ and r_- is critical for the overall performance of the method. Several other implementation issues, such as how to solve the nonlinear equations arising from applying the Gauss method to the regularized equations, still need to be addressed. Also, the proposed algorithms for solving few-body close encounters must be studied more thoroughly and tested numerically. These and other issues will be addressed in a forthcoming article. However, the preliminary results given in this article are very promising, and more than justify further work on the topic.

Acknowledgments. The idea of this paper came up while the second author was a visitor at the Mathematical Sciences Research Institute, Berkeley, CA, during the fall 1998. Research at MSRI is supported in part by NSF grant #DMS 9701755. The second author was also supported by NSF Grant #DMS 9627330. The first author worked on this project during a sabbatical visit

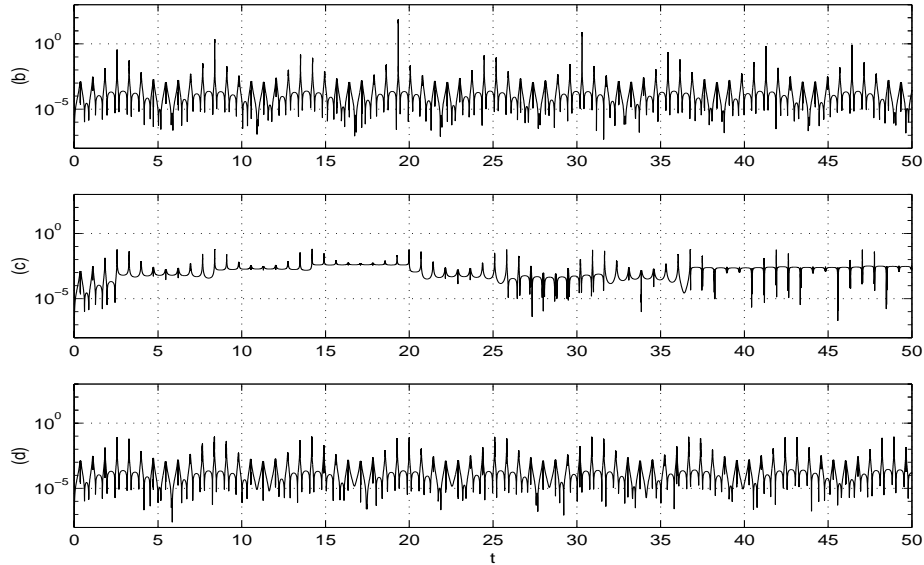


FIGURE 8. The relative energy error for the adaptive methods (b) without switch, (c) with improved hard switch and (d) with smooth switch.

at the University of Kansas. She was supported by the Norwegian Research Council through the SYNODE-II project, contract no. 127582/410.

The authors would also like to thank Marvin McNett (KU) for many fruitful discussions during the work, and Martin Lo (NASA JPL) for his encouragement at the start of the project.

REFERENCES

- [1] Aarseth, S.J., Direct methods for N-body simulation, in *Multiple Time Scales*, eds. J.U. Brackbill and B.I. Cohen, Academic Press, NY, 1985.
- [2] Bond, S., and Leimkuhler, B., Time-transformations for reversible variable stepsize integration, *Numerical Algorithms*. **19**, 55-71, 1998.
- [3] Calvo, M.P. and Sanz-Serna, J.M., The development of variable stepsize symplectic integrators with applications to the two-body problem, *SIAM J. Sci. Comput.* **14**, 936-952, 1993.
- [4] Cooper, G.J., Stability of Runge-Kutta methods for trajectory problems, *IMA J. Numer. Anal.* **7**, 1-13, 1987.
- [5] Goldstein, H., *Classical Mechanics*, 2nd Ed., Addison Wesley, New York, 1980.
- [6] Gu, Y. and Yuan, J.-M., Chaotic scattering of electrons with He^+ , *Phys. Rev.* **A 47**, R2442-R2445, 1993.
- [7] Hairer, E., Norsett, S.P., and Wanner, G., *Solving Ordinary Differential Equations I, Nonstiff Problems*, 2nd Ed., Springer, 1994.
- [8] E. Hairer and G. Wanner. *Solving Ordinary Differential Equations II, Stiff and Differential-Algebraic Problems*, 2nd Ed., Springer, 1996.

- [9] Heggie, D.C., The N-body problem in stellar dynamics, in *Long-Term Dynamical Behavior of Natural and Artificial N-Body Systems*, Ed. A.E. Roy, NATO ASI Series, Kluwer, Dordrecht, 1988.
- [10] Holder, T., Leimkuhler, B., and Reich, S., Explicit variable stepsize and time-reversible integration, preprint, 1998.
- [11] Hut, P., Makino, J., McMillan, S., Building a better leapfrog, *The Astrophysical Journal* **443**, L93-L96, 1995.
- [12] Huang, W., and Leimkuhler, B., The Adaptive Verlet Method, *SIAM J. Sci. Comput.* **18**, 239-256, 1997.
- [13] Hut, P., Funato, Y., Kokubo, E., Makino, J., McMillan, S., Time symmetrization meta-algorithms, in *Computational Astrophysics*, Proc. of the 12th 'Kingston meeting' on Theoretical Astrophysics, Eds. D.A. Clarke and M.J. West, ASP Conf. Series. to appear.
- [14] Budd, C.J. and Iserles, A., Geometric integration: numerical solution of differential equations on manifolds, Numerical Analysis Reports, DAMTP 1998/NA10, University of Cambridge, 1998.
- [15] Leimkuhler, B., Reversible adaptive regularization: perturbed Kepler motion and classical atomic trajectories, *Trans. Roy Soc.*, to appear.
- [16] Klein, M., and Knauf, A., Classical planar scattering by Coulombic potentials, *Lecture Notes in Physics* **13**, Springer-Verlag, Berlin, 1992.
- [17] Landau, L.D., and Lifshitz, E.M., *Mechanics (Course in Theoretical Physics, Vol. 1)*, 3rd Ed., Pergamon Press, Oxford, 1976.
- [18] Marsden, J., *Lectures on Mechanics*, Cambridge University Press, Cambridge, 1992.
- [19] McLachlan, R., On the numerical integration of ordinary differential equations by symmetric composition methods, *SIAM J. Sci. Comp.*, **16**, 151-168, 1995.
- [20] Mikkola, S., A practical and regular formulation of the N-body equations, *Mon. Not. R. Astr. Soc.*, **215**, 171-177, 1985.
- [21] Mikkola, S., A cubic approximation for Kepler's equation. *Celestial Mechanics and Dynamical Astronomy* **40**, 303-312, 1987.
- [22] Nijerhuis, A., Solving Kepler's equation with high efficiency and accuracy, *Celestial Mechanics and Dynamical Astronomy* **51**, 319-330, 1991.
- [23] S.J. Peale, Some unsolved problems in evolutionary dynamics, *Celestial Mechanics and Dynamical Astronomy* **46**, 253-275, 1989.
- [24] Rzazewski, K., Lewenstein, M., and Salieres, P., Multielectron stabilization of atoms in a laser field: classical perspective, *Phys. Rev. A* **49**, 1196-1201, 1994.
- [25] Sanz-Serna, J.M. and Calvo, M.P., *Numerical Hamiltonian Problems*, Chapman and Hall, 1994.
- [26] Skeel, R.D. and Biesidecki, J., Symplectic integration with variable stepsize, *Annals of Numerical Mathematics*, **1**, 191-198, 1994.
- [27] Steckel, J., and Jaffe, C., The bifurcations of the Langmuir orbit in the two-electron atom, *Hamiltonian systems with three or more degrees of freedom*, NATO ASI Series, Kluwer, Dordrecht, 1998.
- [28] Stoffer, D., Variable steps for reversible integration methods, *Computing* **55**, 1-22, 1995.
- [29] Tuckerman, M., Berne, B.J. and Martyna, G.J., Reversible multiple time scale molecular dynamics, *J. Chem. Phys.* **97**, 1990-2001 (1992).
- [30] Verlet, L., Computer experiments on classical fluids I. Thermodynamical properties of Lennard-Jones molecules, *Physical Review* **159**, 98-103 (1967).
- [31] Wisdom, J. and Holman, M., Symplectic maps for the N-body problem, *The Astronomical Journal* **102**, 1528-1538, 1991.
- [32] Yoshida, H., Construction of higher order symplectic integrators, *Phys. Lett. A* **150**, 262-268, 1990.